

Analysis of Hydrocarbons in the Exhaust Gas of a Fusion Test Device Using Infrared Absorption Spectroscopy^{*)}

Masahiro TANAKA^{1,2)}, Hiromi KATO¹⁾ and Naoyuki SUZUKI¹⁾

¹⁾National Institute for Fusion Science, 322-6 Oroshi-cho, Toki, Gifu 509-5292, Japan

²⁾The Graduate University for Advanced Studies, SOKENDAI, 322-6 Oroshi-cho, Toki, Gifu 509-5292, Japan

(Received 29 November 2019 / Accepted 5 February 2020)

To investigate the behavior of hydrogen isotopes in a large fusion test device, a new technique using infrared absorption spectroscopy is applied for the monitoring of hydrocarbons in exhaust gas. Fourier transform infrared (FT-IR) spectroscopy combined with a gas cell, which has an optical path length of 16 m, was installed at the plasma exhaust line. In this configuration, the detection limit of CH₄, C₂H₆, C₂H₄, and CO is at the level of sub-ppm. The exhaust gas observations were conducted during hydrogen glow discharge and during the regeneration operation of cryosorption pumps during the hydrogen plasma phase. As a result, hydrocarbons and carbon monoxide were detected in the exhaust gas, and the exhaust behavior and the ratio of gas components were determined. It is also demonstrated that light and the heavy hydrocarbons can be discriminated by the FT-IR system. Our infrared absorption spectroscopy study provides positive prospects for its application to exhaust gas analyses.

© 2020 The Japan Society of Plasma Science and Nuclear Fusion Research

Keywords: exhaust gas monitoring, hydrocarbons analysis, FT-IR, long optical path gas cell, deuterium plasma experiment, large fusion test device

DOI: 10.1585/pfr.15.2405008

1. Introduction

Understanding the behavior of hydrogen isotopes in fusion test devices is an important issue from the viewpoints of radiation safety, development of the fuel cycle process and for tritium removal systems. To observe the behavior of hydrogen in the exhaust gas from the fusion test devices, various types of analytical gas instruments have been applied [1–10]. One type of conventional gas analysis instrument is a gas chromatograph (GC), which uses a thermal conductivity detector (TCD) and a flame ionization detector. Residual gas analyses are also performed using high-resolution quadrupole mass spectrometry and threshold ionization mass spectrometry. These systems have been applied for gas analyses by teams operating in the JT-60U [1–3, 7], JET [4–6, 8], AUG [9], and EAST [10] experiments. The purpose of a gas analysis instrument is to determine the concentrations of hydrogen isotope gases (Q₂, Q = H, D, T) and impurities including noble gases, air components, and hydrocarbons. Among these gas species, hydrocarbons are produced in fusion test devices via chemical sputtering, especially when the plasma-facing materials are made of carbon. Hydrocarbons have been detected in exhaust gases in experiments at JT-60U and JET by use of GC systems [1–6].

At NIFS, the Large Helical Device (LHD), which has a large superconducting magnet system, has been used to

conduct plasma experiments using hydrogen (H) and deuterium (D) since 2017 [11, 12]. In deuterium plasma experiments, a small amount of tritium is produced by D-D reactions. The tritium is exhausted along with the operation gas, which contains D, H, and other impurities, via a vacuum pumping system. The exhausted tritium from all equipment in LHD is removed by the exhaust detritiation system (EDS) [13]. To determine the tritium activity and its chemical forms, a water bubbler system that can discriminate between different chemical forms of tritium has been developed and installed at the inlet of the EDS [14]. After installation, in the subsequent monitoring results, tritiated hydrocarbons were detected in the exhaust gas. However, the chemical forms of the hydrocarbons could not be detected by the GC and TCD system, which has a detection limit of a few tens ppm.

In this study, to analyze trace components such as hydrocarbons in exhaust gas, we propose a new technique that uses infrared absorption spectroscopy combined with a long optical path gas cell that is applied for the monitoring of exhaust gas during glow discharge cleaning operations and the regeneration operation of cryosorption pumps in the LHD.

2. Experimental Setup

2.1 FT-IR and gas sampling system

In this study, infrared absorption spectra were obtained by our Fourier transform infrared (FT-IR) spectroscopy system. A schematic diagram of the analytical

author's e-mail: tanaka.masahiro@nifs.ac.jp

^{*)} This article is based on the presentation at the 28th International Toki Conference on Plasma and Fusion Research (ITC28).

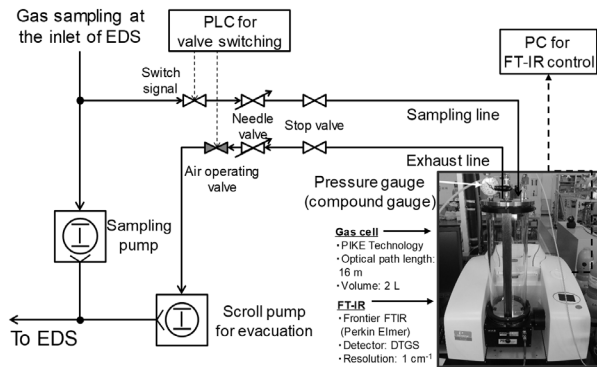


Fig. 1 Schematic diagram of the FT-IR system.

system is shown in Fig. 1, which consists of an FT-IR spectroscope (Frontier FT-IR, Perkin Elmer) combined with a long optical path gas cell (optical path length: 1–16 m (variable), cell volume: 2 L, PIKE Technologies, PN: 163-1674), and a remote gas sampling system that uses a programmable logic controller. To reduce the effect of CO_2 and H_2O absorption, the optical passes in the FT-IR instruments and the gas cell system are swept by dry N_2 . During the experiments, the scan numbers were set to 50 or 80, the wave number resolution was set to 1 cm^{-1} , and the optical path length was fixed to 16 m. The Atmospheric Vapor Compensation algorithm, which is an advanced digital filtering algorithm designed to compensate for CO_2 and H_2O absorption [15], was used when obtaining the measurements. Deuterated triglycine sulfate was used as a photo detector at room temperature. Optical windows made of KBr were used for the FT-IR instruments and the gas cell system. Since the dew point in the sample gas was below -20°C , there were negligible moisture effects in the KBr window.

The remote gas sampling apparatus for the FT-IR system was connected to an inlet of the EDS. The remote gas sampling system consisted of a pump for gas sampling, a scroll pump for evacuation of the gas cell, needle valves for the adjusting gas flow rate, an air operating valve that allows for modification of the operational mode of gas filling and evacuation of the gas cell, and a compound pressure gage to monitor the pressure in the gas cell. The gas sampling flow rate was about 0.4 L/min. The following operational sequence was employed: (1) Evacuation of the gas cell to less than -95 kPa (G) (for 5 or 6 min), (2) filling up the gas cell with the sample gas to atmospheric pressure (for 5 or 8 min), and (3) measurements made with the FT-IR system (for 15 or 22 min). The total measurement interval was either 25 min or 36 min.

2.2 FT-IR spectrum and calibration

Figure 2 shows an example FT-IR spectrum obtained during the molecular hydrogen (H_2) glow discharge cleaning operation in the LHD. The number of scans was 80. The signal indicates the absorbance which was obtained after subtraction of the background signal. In this spec-

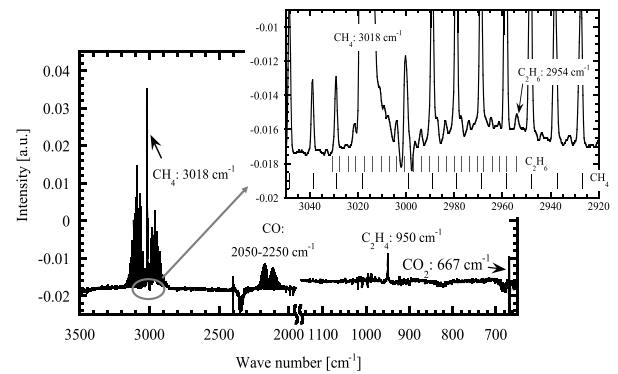


Fig. 2 An example FT-IR spectrum obtained during the H_2 glow discharge cleaning operation in the LHD. The vertical bars in the sub graph represent the absorption lines of C_2H_6 and CH_4 .

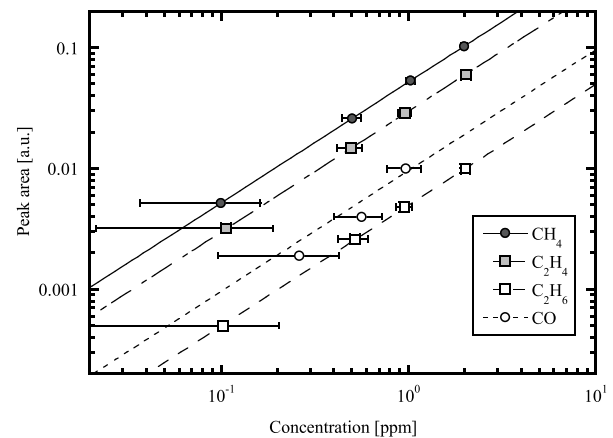


Fig. 3 Correlation between the standard gas concentrations and the peak areas.

trum, the background gas used the exhaust gas to eliminate the signal of impurity gases such as CO_2 . The background spectra were obtained once a day before starting the plasma experiment. The different gas species were identified in the absorption spectra in consultation with previous works [16–20], where methane, ethane, ethylene, carbon dioxide, and carbon monoxide were detected in the exhaust gas. The identification peaks of methane, ethylene, carbon dioxide and carbon monoxide were 3018 cm^{-1} , 950 cm^{-1} , 667 cm^{-1} and 2172 cm^{-1} , respectively. A peak attributed to ethane at 2954 cm^{-1} was observed between two absorption peaks of methane, as shown in Fig. 2. This small peak was used for the identification and calibration of ethane.

Figure 3 shows the correlation results of methane, ethane, ethylene, and carbon monoxide. Dry nitrogen gas was used for the background spectrum measurements. A mixture containing 1 ppm of carbon monoxide and 2 ppm of methane, ethylene, and ethane relative to the nitrogen gas was used as the standard gas. To achieve a calibration in the sub-ppm range, the standard gas was prepared by the manometric blending (diluting) method using ultrahigh-purity (UHP) N_2 gas (99.99995% purity). First, the stan-

Table 1 The calibration conditions and results calculated by the Spectrum Quant software.

Gas species	Peak wave number (cm ⁻¹)	Range of baseline for peak area calculation (cm ⁻¹)	Linear regression coefficient
CH ₄	3018	3010 ~ 3020	1.000
C ₂ H ₄	950	944 ~ 954	1.000
C ₂ H ₆	2954	2952 ~ 2956	0.999
CO	2172	2171 ~ 2174	0.992

ard gas was filled into the gas cell, which was evacuated to less than -95 kPa (G), until it reached atmospheric pressure. Next, the gas was evacuated until it reached the pre-designated pressure and then UHP N₂ was filled into the gas cell until it reached atmospheric pressure. The concentration in the blending gas was calculated using the ratio of the designated pressure and the atmospheric pressure after dilution. The blending accuracy at the 0.1-ppm level is typically a few tens of % of the relative proportion value due to the accuracy of the pressure gage and gas-compressibility factors. The calibration method employed Beer's law and was conducted with the Spectrum Quant software (Perkin Elmer). The peak area for calibration was defined as a region enclosed by the signal curve and the baseline which connected the lowest point at both sides of a peak. The detail calibration condition and results are summarized in Table 1. The detection limit among these chemical species was close to 0.1 ppm in these operational conditions.

3. Results and Discussion

3.1 Monitoring results in the exhaust gas of glow discharge and regeneration of the cryosorption pump

The analysis of hydrocarbons in the exhaust gas was conducted in the H₂ plasma phase. The background spectrum was measured before starting the plasma experiment each day. Carbon dioxide was always observed at about a few tens ppm in the exhaust gas because some air in the room would be mixed into the exhaust gas line. However, the behavior of carbon dioxide in the exhaust gas is not discussed in this paper. Figure 4 shows the behavior of the hydrocarbons and carbon monoxide during the hydrogen and helium glow discharge cleaning operations, the operational conditions of which are summarized in Table 2. During these operations, two electrodes in the glow discharge system were exchanged once every hour. During the helium glow discharge process, the main gas component was carbon monoxide. Helium plasma sputtered the first wall and then oxygen would be released from the stainless steel and react with carbon. Hydrocarbons were also observed. Since a small amount of hydrogen gas was detected in the exhaust gas, the hydrocarbons were produced in the LHD vacuum vessel. The amount of hydrocarbons increased during hydrogen glow discharge process. Hydrocarbons

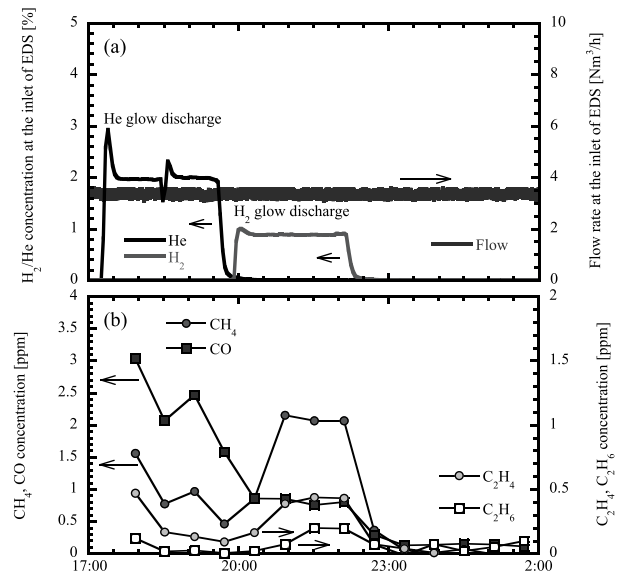


Fig. 4 Variations of the gas species in the exhaust gas during the helium and H₂ glow discharge cleaning operations: (a) Concentrations of hydrogen, helium and the exhaust gas flow, and (b) concentrations of the hydrocarbons and carbon monoxide.

Table 2 Summary of the glow-discharge operation conditions shown in Fig. 4.

Gases	Electrode No.	Current	Voltage	Pressure	Discharge period
He	G1	15 A	261 V	0.84 Pa	1 h
	G2	15 A	268 V	0.84 Pa	1 h
H ₂	G1	10 A	332 V	0.67 Pa	1 h
	G2	10 A	355 V	0.67 Pa	1 h

were generated by the chemical sputtering in the hydrogen plasma.

Figure 5 shows the variation of hydrogen, hydrocarbons and carbon monoxide during the regeneration operation of the cryosorption pump for the Neutral Beam Injection (NBI) system and the Closed Helical Divertor (CHD). The regeneration operation was conducted on the last day of the H₂ plasma experiments. The observed gas species and concentrations in the regeneration operation of the NBI and CHD cryosorption pumps indicated the results of the plasma operation. The cryosorption pumps were operated at 77 K. The regeneration operations for NBI #4 and #5 were started at 13:00, and then those for NBI #1, #2, and #3 were done from 18:30. The regeneration operation of CHD was conducted from 20:30 following the regeneration operations for all NBIs. Hydrogen gas was released from the cryosorption pump first. Methane and carbon monoxide were released a few hours after the hydrogen gas was released. Ethane and ethylene then were released about 10 hours later. These release behaviors indicate that the desorption process from the cryosorption

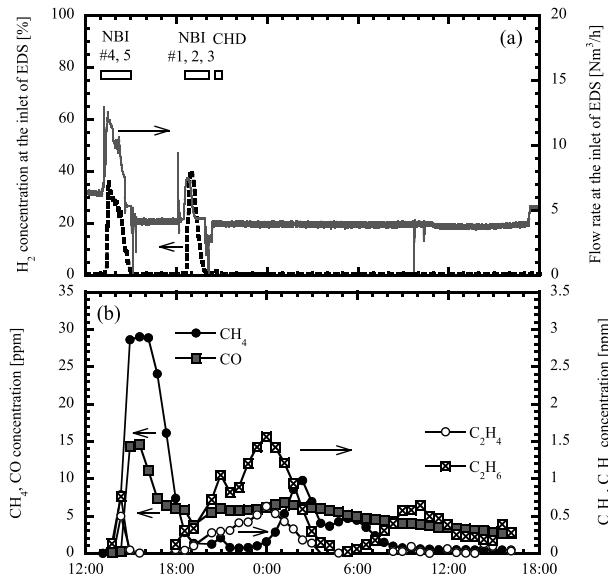


Fig. 5 Variations of the gas species in the exhaust gas during the regeneration operation of the cryosorption pump for the NBI and CHD: (a) Concentrations of hydrogen and the exhaust gas flow, and (b) concentrations of the hydrocarbons and carbon monoxide.

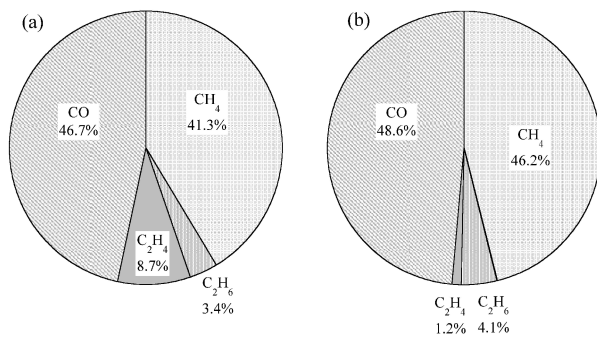


Fig. 6 The ratio of gas species in the exhaust gas: (a) Glow discharge cleaning operation, and (b) regeneration operation of cryosorption pumps for the NBI and CHD.

pump depends on the temperature of the absorbent. Along these lines, Fukada *et al.* investigated the desorption rate of a mixture of He, H₂, and CH₄ absorbed by activated carbon in temperatures ranging from 10 K to room temperature. The temperatures at the time when desorption started were 20 K for He, 75 K for H₂, and 180 K for CH₄ [21]. The observation results obtained in this study are shown in Fig. 5, which suggest that the desorption temperatures of ethane and ethylene may be more than 180 K. It was also observed that carbon monoxide was released on a continual basis; the reason for this continuous release is not yet clear.

Figure 6 shows the ratios of the different gas species in the exhaust gas during the glow discharge cleaning operations and the regeneration operation of the cryosorption pumps. The ratio of carbon monoxide in both operations

Table 3 The absorption wave number of H and D in hydrocarbons [20].

Chemical forms (Q=H, D)	Wave number (cm ⁻¹)		Type of mode
	H	D	
Methane (CQ ₄)	3018.9	2259	degenerate stretching
Ethane (C ₂ Q ₆)	2954	2083	symmetrical stretching
Ethylene (C ₂ Q ₄)	949.3	720	CQ ₂ wagging vibration
Acetylene (C ₂ Q ₂)	730.3	536.9	CQ bending

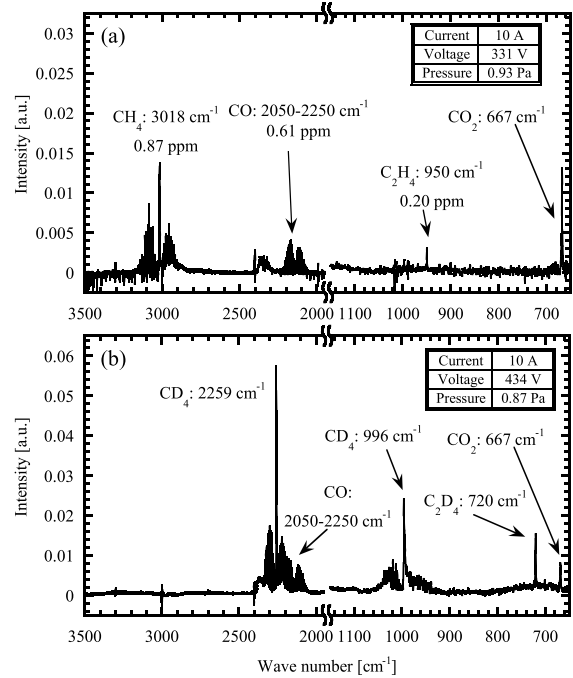


Fig. 7 FT-IR spectrum of the exhaust gas during the glow discharge cleaning operation. The conditions of glow discharge cleaning are shown in each graph. (a) H₂ glow discharge, and (b) D₂ glow discharge.

was found to be the highest, while that of methane was almost the same as that of carbon monoxide. On the other hand, the ratio of ethane and ethylene were only a few % and their yields were less than that of methane. The ratios of gas species in the LHD are similar to the results found from the JT-60U [2]. Although the types of devices in both experimental apparatuses are different, the carbon tiles employed as the plasma-facing material are used in both the LHD and JT-60U experiments. Thus, this might suggest that the plasma parameters in the edge plasma regions in both devices are almost the same.

3.2 Hydrogen isotope effect of the hydrocarbons in FT-IR system

The absorption wave number of H and D in the hydrocarbons are summarized in Table 3. The absorption wave numbers of the hydrocarbons shifted to lower values when H was replaced with D. Figure 7 shows a FT-IR spectrum of the exhaust gas during the hydrogen and deuterium glow

discharge cleaning operations. The figure indicates that the absorption features attributed to CD_4 and C_2D_4 can be discriminated from those of CH_4 and C_2H_4 . Discrimination measurements of H and D in the hydrocarbons were successfully achieved by our FT-IR system.

4. Summary

A FT-IR system combined with a long optical path gas cell was applied for the analysis of hydrocarbons in exhaust gases. Hydrocarbons such as methane, ethane, ethylene, and carbon monoxide were detected during H_2 glow discharge cleaning operations and the regeneration operation of cryosorption pumps in the H_2 plasma phase. Our results suggest that the infrared absorption spectroscopy technique has positive prospects for analyses of exhaust gases from fusion test devices.

Acknowledgments

This study was supported by the NIFS budget NIFS18ULAA023, and JSPS KAKENHI Grant Number 17K06998 and 18H01204.

- [1] H. Nakamura *et al.*, Fusion Eng. Des. **70**, 163 (2004).
- [2] K. Isobe *et al.*, Fusion Eng. Des. **81**, 827 (2006).
- [3] A. Kaminaga *et al.*, Proc. of 20th IEEE/NPSS SOFE, 2003, pp. 144-147.
- [4] S. Grünhagen *et al.*, Fusion Sci. Technol. **60**, 931 (2011).
- [5] S. Grünhagen Romanelli *et al.*, Phys. Scr. **T159**, 014068 (2014).
- [6] S.G. Romanelli *et al.*, Fusion Sci. Technol. **71**, 467 (2017).
- [7] T. Hayashi *et al.*, Fusion Eng. Des. **84**, 908 (2009).
- [8] U. Kruezi *et al.*, Rev. Sci. Instrum. **83**, 10D728 (2012).
- [9] D. Neuwirth *et al.*, Plasma Phys. Control. Fusion **54**, 085008 (2012).
- [10] J. Wang *et al.*, Vacuum **167**, 98 (2019).
- [11] M. Osakabe *et al.*, Fusion Sci. Technol. **72**, 199 (2017).
- [12] M. Osakabe *et al.*, IEEE Trans. Plasma Sci. **46**, 2324 (2018).
- [13] M. Tanaka *et al.*, Fusion Eng. Des. **127**, 275 (2018).
- [14] M. Tanaka *et al.*, J. Radioanal. Nucl. Chem. **318**, 877 (2018).
- [15] Perkin Elmer Frontier catalogue (2011).
- [16] L.G. Smith, J. Chem. Phys. **17**, 139 (1949).
- [17] H.W. Thompson, *Tables of Wavenumbers for the Calibration of Infra-red Spectrometers* (BUTTER WORTHS, London, 1961).
- [18] E.K. Plyler *et al.*, J. Res. Nat. Bur. Stand. A **64**, 29 (1960).
- [19] J.N. Gayles, Jr. and W.T. King, Spectrochim. Acta **21**, 543 (1965).
- [20] T. Shimanouchi, "Tables of molecular vibrational frequencies consolidated volume I", Nat. Stand. Ref. Data Ser., Nat. Bur. Stand. (U.S.), 39 (1972).
- [21] S. Fukada and M. Terashita, J. Nucl. Sci. Technol. **47**, 1219 (2010).